FERMILAB-PUB-16-470-A

Prepared for submission to JCAP

arXiv:1610.07587v1 [astro-ph.HE] 24 Oct 2016

Gamma Rays From Dark Matter Subhalos Revisited: Refining the Predictions and Constraints

Dan Hooper[a,b,c] **and Samuel J. Witte**[a,d]

[a]Fermi National Accelerator Laboratory, Center for Particle Astrophysics, Batavia, IL 60510
[b]University of Chicago, Department of Astronomy and Astrophysics, Chicago, IL 60637
[c]University of Chicago, Kavli Institute for Cosmological Physics, Chicago, IL 60637
[d]University of California, Los Angeles, Department of Physics and Astronomy, Los Angeles, CA 90095

E-mail: dhooper@fnal.gov, switte@physics.ucla.edu

Abstract. Utilizing data from the ELVIS and Via Lactea-II simulations, we characterize the local dark matter subhalo population, and use this information to refine the predictions for the gamma-ray fluxes arising from annihilating dark matter in this class of objects. We find that the shapes of nearby subhalos are significantly altered by tidal effects, and are generally not well described by NFW density profiles, instead prefering power-law profiles with an exponential cutoff. From the subhalo candidates detected by the Fermi Gamma-Ray Space Telescope, we place limits on the dark matter annihilation cross section that are only modestly weaker than those based on observations of dwarf galaxies. We also calculate the fraction of observable subhalos that are predicted to be spatially extended at a level potentially discernible to Fermi.

[1]ORCID: http://orcid.org/0000-0001-8837-4127
[2]ORCID: http://orcid.org/0000-0001-4649-3085

Contents

1 Introduction **1**

2 Subhalo Populations in Cosmological Simulations **2**
2.1 The Via Lactea II and ELVIS Simulations 2
2.2 The Dark Matter Profiles of Simulated Subhalos 3

3 Detecting Dark Matter Subhalos With Gamma-Ray Telescopes **9**
3.1 Gamma-Rays from Dark Matter Subhalos 9
3.2 Placing Constraints on the Dark Matter Annihilation Cross Section 9
3.3 Prospects for Detecting Spatial Extension 10
3.4 Uncertainties 14

4 Summary and Conclusion **16**

1 Introduction

A wide range of experimental strategies are being pursued in an effort to observe dark matter's non-gravitational interactions and ultimately identify the particle nature of dark matter. This program includes but is not limited to experiments designed to detect the scattering of dark matter with nuclei, searches for the annihilation or decay products of dark matter, and efforts to produce and observe dark matter at accelerators. In all three of these areas, current experiments are probing important regions of parameter space and are sensitive to a wide range of well motivated dark matter candidates.

Particularly promising are searches for dark matter utilizing gamma-ray telescopes. Constraints from the Fermi Gamma-Ray Space Telescope's observations of dwarf spheroidal galaxies [1, 2], the Galactic Center [3] and the extragalactic gamma-ray background [4, 5], are each currently sensitive to dark matter particles with masses in the range of ∼10-100 GeV and annihilation cross sections similar to that naively predicted from thermal relic abundance considerations, $\sigma v \simeq 2 \times 10^{-26}$ cm^3/s. Furthermore, the excess of GeV-scale gamma rays observed from the region surrounding the Galactic Center exhibits a spectrum and morphology that is consistent with the predictions of dark matter particles with a mass of $\sim 30-60$ GeV and an annihilation cross section of $\sigma v \sim 10^{-26}$ cm^3/s [6–15] (for discussions of other interpretations, see Refs. [16–25]).

Within the standard paradigm of cold and collisionless dark matter, structure forms hierarchically, meaning that the smallest halos form first and gradually merge to form larger systems, including the halos that host galaxies and galaxy clusters [26]. As a consequence of this process, the dark matter halos that encompass galaxies are predicted to contain large numbers of smaller subhalos.

In the case of the Milky Way, the largest and most massive subhalos include the known dwarf galaxies, as well as the Large and Small Magellanic Clouds. This collection of very massive objects reflects only a small fraction of the subhalo population, however. A much larger number of subhalos that are too small to capture significant quantities of gas and form stars are also expected to be present, while remaining invisible to surveys at optical and other wavelengths. If dark matter particles annihilate with a cross section that is similar to

that naively predicted for a thermal relic, nearby subhalos could be a promising target for gamma-ray telescopes [27–44].

The most recent catalog released by the Fermi Collaboration (the 3FGL) contains 992 gamma-ray sources that have not been associated with emission observed at other wavelengths [45], a small fraction of which could potentially be dark matter subhalos. Recent studies of the 3FGL identified a subset of 19 bright ($\Phi_\gamma > 7 \times 10^{-10}$ cm^{-2} s^{-1}, $E_\gamma > 1$ GeV) and high-latitude ($|b| > 20^\circ$) sources that show no evidence of variability and exhibit a spectral shape that is consistent with the predictions of annihilating dark matter [27, 28]. From the characteristics of these subhalo candidate sources, limits can be derived on the dark matter annihilation cross section. Such limits, however, can vary significantly depending on the assumptions that are made regarding the local abundance of dark matter subhalos and on the spatial distribution of dark matter within these systems. For example, the limits on the dark matter's annihilation cross section placed in Ref. [27] and Ref. [29] differ by a factor of a few for most dark matter masses, resulting largely from differences in the assumed subhalo density profiles. More specifically, whereas the authors of Ref. [27] adopted density profiles that are described by an Einasto profile, tidally truncated to remove the outermost 99.5% of a given subhalo's mass, Ref. [29] chose instead to adopt a traditional NFW density profile, with concentrations chosen to match the parameters of a given subhalo identified within the Via Lactea II simulation. In reality, however, it is likely that the true population of nearby subhalos is not particularly well described by either of these simple halo profile parameterizations.

In this paper, we revisit the characteristics of the local dark matter subhalo population, basing our analysis on the properties of the subhalos identified within the cosmological simulations Via Lactea II and ELVIS. We find that the simulated subhalos in the local region of the Milky Way are generally well characterized by power-law density profiles with an exponential cutoff. Using this profile parameterization, and accounting for halo-to-halo variations as determined by the distribution of simulated subhalos, we estimate the number of subhalos that could be observed by the Fermi Large Area Telescope (Fermi-LAT) and use this information to place constraints on the dark matter's annihilation cross section. We also calculate the fraction of the observable subhalos that will be spatially extended at a level potentially discernible to experiments such as Fermi, providing us with a way of discriminating a dark matter subhalo population from a collection of point-like gamma-ray sources.

2 Subhalo Populations in Cosmological Simulations

2.1 The Via Lactea II and ELVIS Simulations

In an effort to characterize the population of dark matter subhalos located within the local volume of the Milky Way, we utilize the publicly available data from the Via Lactea II (VL-II) [46] and ELVIS [47] cosmological simulations. The VL-II simulation contains over 1 billion particles, each with a mass of $4.1 \times 10^3 M_\odot$, and identifies approximately 20,000 subhalos with a maximum circular velocity, $v_{c,\rm max}$, greater than 4 km/s. Since we are interested here in subhalos residing within Milky Way-like halos, we have chosen to restrict our attention to those subhalos that are located within 300 kiloparsecs (kpc) of the center of the host halo. Furthermore, in order to minimize the impact of thresholds and other ambiguities associated with subhalo identification and characterization, we limit our analysis to those subhalos that consist of 100 or more particles. These cuts reduce the number of VL-II subhalos used in our analysis to 5,268.

The ELVIS suite consists of 48 simulated halos, each comprised of at least 53 million particles with masses of $1.9 \times 10^5 M_\odot$. Half of these simulations are of paired galaxies, intended to be representative of the Milky Way-Andromeda system in both mass and phase space. Three high-resolution simulations were performed on isolated halos (in addition to the aforementioned 48) with a particle mass of $2.35 \times 10^4 M_\odot$. In our analysis, we consider those subhalos that are comprised of at least 100 particles and with $v_{c,\rm max} > 8$ km/s in the paired and isolated simulations, and $v_{c,\rm max} > 4$ km/s in the high-resolution simulations. As with VL-II, we have restricted our attention to subhalos that are located within 300 kpc of the nearest host halo's center, leaving us with a total of 26,048 subhalos from among the suite of ELVIS simulations.

For each subhalo found in either simulation catalogue, we extract $v_{c,\rm max}$, the radius at which maximum circular velocity occurs, $R_{v,\rm max}$, and the total gravitationally bound mass (each evaluated at $z = 0$). It is well known that the velocity profiles and concentrations of the subhalos extracted from dark matter simulations depend on the precise values of the adopted cosmological parameters. Ref. [48] derived a scaling relation for $R_{v,\rm max}$ (at fixed $v_{c,\rm max}$) on the cosmological parameters σ_8 and n_s, based on the results of various cold DM simulations. Specifically, they found the following:

$$R_{v,\rm max} \propto (\sigma_8\, 5.5^{n_s})^{-1.5}\,. \tag{2.1}$$

Since the cosmological parameters adopted by VL-II and ELVIS are based on WMAP-3 ($\sigma_8 = 0.74$, $n_s = 0.951$) and WMAP-7 ($\sigma_8 = 0.80$, $n_s = 0.963$), respectively, we have rescaled both to the latest results from the Planck Collaboration ($\sigma_8 = 0.82$, $n_s = 0.967$) [49].

2.2 The Dark Matter Profiles of Simulated Subhalos

Various groups have utilized Fermi's catalog of unassociated gamma-ray sources to derive limits on the dark matter annihilation cross section [27, 29, 30, 50]. The results of these studies, however, vary considerably depending on the assumed characteristics of the local subhalo population. With this in mind, we have investigated the distribution of dark matter in subhalos identified within the VL-II and ELVIS simulations. Specifically, for each subhalo, we considered various parameterizations of the density profile and determined which can provide good agreement with the simulated values of $v_{c,\rm max}$, $R_{v,\rm max}$, and the total gravitationally bound mass.[1]

After determining that the subhalo profile parameterizations adopted in both Refs. [27, 30] and Ref. [29] provide poor fits to the subhalos located near the center of the host halo, we further considered a doubly-generalized NFW profile of the following form:

$$\rho(r) = \frac{\rho_s}{\left(\frac{r}{r_s}\right)^{\gamma_1}\left(\frac{r}{r_s}+1\right)^{\gamma_2}}, \tag{2.2}$$

where the case of a canonical NFW profile is recovered for $\gamma_1 = 1$ and $\gamma_2 = 2$. For those subhalos located in the outer regions of a host halo, we found that this parameterization could in most cases be tuned to match the characteristics found in the simulations. But for subhalos located within the innermost few tens of kiloparsecs of their host halo, we found that this class of profile shapes could generally *not* simultaneously accommodate both the

[1] Although we would ideally like to extract information for the $r < R_{v,\rm max}$ region of a given subhalo, statistical limitations make this impractical in most cases. We focus here on the values of the more reliably determined quantities, $v_{c,\rm max}$, $R_{v,\rm max}$, and $M_{\rm tot}$.

mass contained within $R_{v,\rm max}$ (i.e. $M(< R_{v,\rm max})$) and the total mass, $M_{\rm tot}$, of the subhalo (for any profile with $\gamma_1 > 0$). We attribute the inability of the doubly-generalized NFW profile to describe these subhalos to the effects of tidal stripping, which are more pronounced in high density environments.

Next, inspired by Ref. [51] (see also Ref. [52]), we considered the following density profile for the local population of tidally truncated subhalos:

$$\rho(r) = \frac{\rho_0}{r^\gamma} \exp\left(-\frac{r}{R_b}\right). \tag{2.3}$$

For nearly all of the simulated subhalos considered in this analysis, we are able to identify choices of γ and R_b that can simultaneously accommodate the reported values of both $M(< R_{v,\rm max})$ and $M_{\rm tot}$.

Our goal in this work is to identify the properties and distributions of the local subhalo population. Unfortunately, there are simply not enough subhalos in the inner tens of kiloparsecs to meaningfully extract properties exclusively from this sample. We approached this problem by identifying trends in the behavior of the best-fit values of γ and R_b as functions of the total subhalo mass and the distance to the center of the host halo. This was accomplished by dividing subhalos into four mass bins, and then dividing each mass bin into four bins that differentiate halos by their distance to the Galactic Center. Bin sizes were chosen in such a way that each bin contains an approximately equal number of subhalos. Scatter plots of these best-fit values are shown in Figs. 1 and 2.

As the result of tidal stripping, one can see in Fig. 2 that the average value of R_b decreases with proximity to the center of the host halo. This result is consistent, for example, with the recent findings of Ref. [53]. Perhaps less anticipated is that the average inner slope, γ, is also found to be lower for those subhalos located near the Galactic Center.

To parameterize the distribution of the values of γ at Earth's location, we adopt a generalized normal distribution:

$$\frac{dP}{d\gamma} = \frac{1}{\sigma\sqrt{2\pi}} \frac{1}{\sigma - \kappa(\gamma - \langle\gamma\rangle)} \exp\left(-\frac{(\gamma - \langle\gamma\rangle)^2}{2\sigma^2}\right), \tag{2.4}$$

where $\langle\gamma\rangle$ is the median value of γ, and σ and κ describe the width and skew of the distribution. For each bin in subhalo mass and Galactic Center distance, we find the values of $\langle\gamma\rangle$, σ and κ which provide the best fit to the simulated dataset. Once these best-fit parameters have been determined, we extrapolate the 68% containment regions of this function to a location 8.5 kpc from the Galactic Center, and use this information to fix the values of $\langle\gamma\rangle$, σ and κ which describe the local subhalo population.

Similarly, to characterize the distribution of R_b we adopt a log-normal distribution:

$$\frac{dP}{dR_b} = \frac{1}{\sigma\sqrt{2\pi}} \frac{1}{R_b} \exp\left(-\frac{(\ln R_b - \ln\langle R_b\rangle)^2}{2\sigma^2}\right), \tag{2.5}$$

where $\langle R_b\rangle$ is the median value of R_b, and σ is the width of the distribution. Once again, we find the values of $\langle R_b\rangle$ and σ which provide the best fit to the simulated dataset in each bin in subhalo mass and Galactic Center distance. As we find that the value of σ is not dependent on the subhalo mass or Galactic Center distance, we average all bins to determine the distribution of R_b. Although one might worry that there could exist correlations between γ and R_b that would limit the validity of our approach, we have found no such correlations

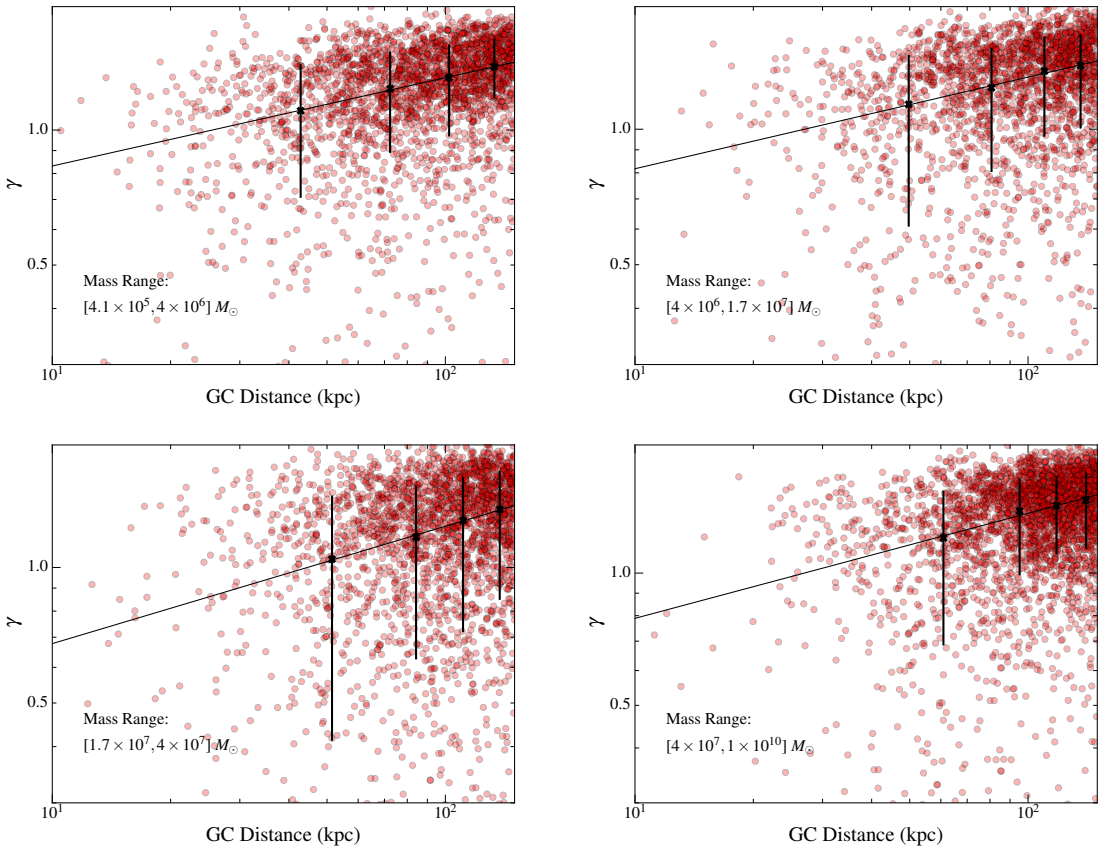

Figure 1. The best-fit values found for the inner slope, γ, for subhalos in the Via Lactea-II and ELVIS simulations, adoping a profile of the form $\rho(r) = \rho_0\, r^{-\gamma} \exp(-r/R_b)$. Results are presented as a function of the distance of the subhalo to the center of the host halo, with each frame corresponding to subhalos in a different mass range. The solid line denotes the power-law trend for the median value of this parameter, while the error bars depict the range of values found among the central 68% of subhalos in each of four distance bins.

to be present in the data. The distributions described by Eqns. 2.4 and 2.5 appear to do an excellent job of capturing the characteristics of the simulated subhalo population.

In Fig. 3, we show examples of the fitted distributions for the case of subhalos with masses in the range of $(2-5) \times 10^7 M_\odot$, for various ranges of the distance to the Galactic Center. In Fig. 4, we plot the distributions of γ and R_b for the local subhalo population, as a function of subhalo mass. We find that the mass dependence of the exponential scale parameter is well described by a power-law, with $\langle R_b(M) \rangle \propto M^{0.421}$. The inner slope, in contrast, appears to be independent of the subhalo mass and favors a median value of $\langle \gamma \rangle \simeq 0.74$. We have verified that our results are relatively insensitive to the choice of binning.

If Fig. 5, we compare the median subhalo density profiles adopted in Ref. [27] (black), Ref. [29] (magenta), and as derived in this study (blue), for subhalos ranging in mass from $10^4 M_\odot$ to $10^7 M_\odot$. As the volume integral of the NFW profile adopted in Ref. [29] yields a subhalo mass that exceeds that reported by VL-II, we take the outer regions of the dark matter distribution to be unspecified in this case. To convey this, we plot this profile as a solid line only within the radius that contains the mass reported by VL-II, and as a dashed

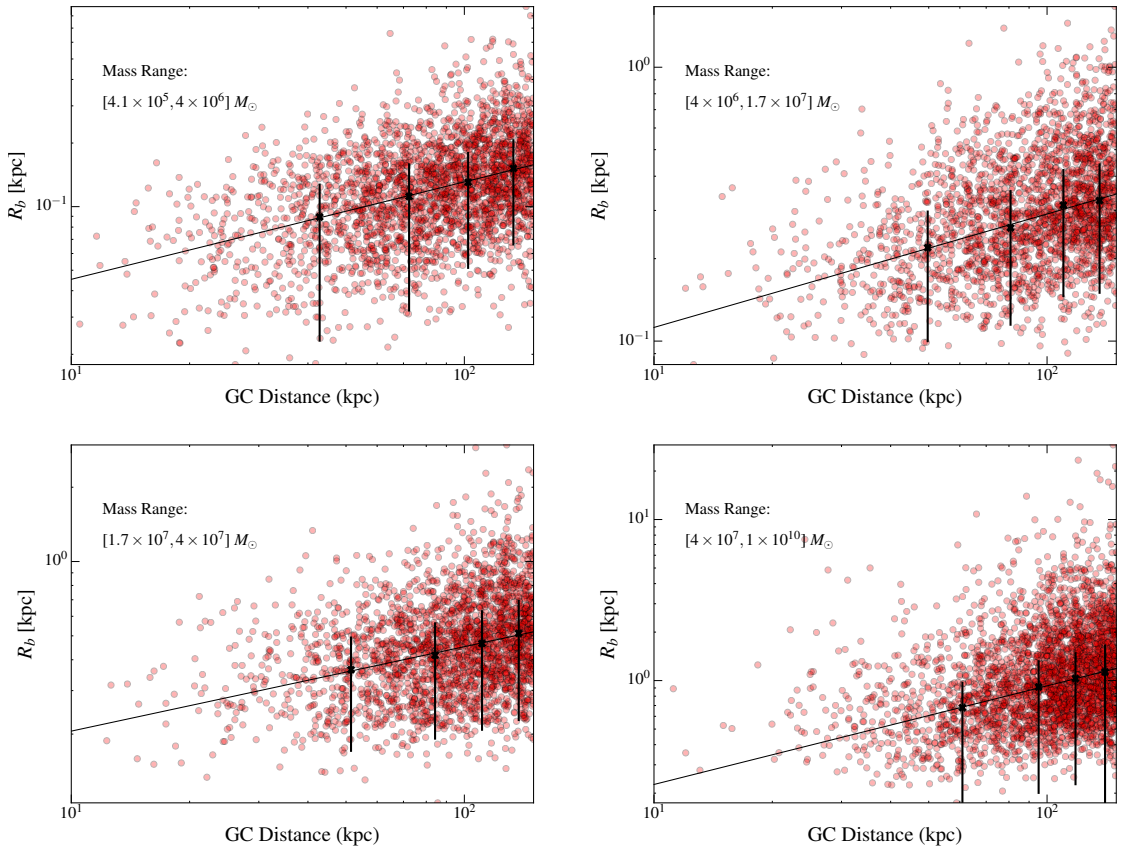

Figure 2. As in Fig. 1, but for the parameter R_b, where $\rho(r) = \rho_0\, r^{-\gamma} \exp(-r/R_b)$. As a result of tidal stripping, the average value of R_b decreases with proximity to the center of the host halo.

line beyond this point.[2]

In order to predict the number of subhalos that could be observed by Fermi-LAT, one needs not only the shapes of the subhalo density profiles, but also the local number density of subhalos of a given mass. In the left panel of Fig. 6, we plot the number of subhalos in the ELVIS simulation per unit subhalo mass as a function of subhalo mass. For masses above $10^8\,M_\odot$, we find that this distribution is well fit by $dN/dM \propto M^{-1.9}$, consistent with previous literature [46, 47, 54, 55]. Although the distribution appears to depart from this power-law at lower masses, we attribute this to the finite resolution of the ELVIS simulation.

In the right panel of Fig. 6, we plot the number density of subhalos as a function of the distance to the host center. Consistent with Refs. [54, 55], we find that this distribution is well-characterized by an Einasto profile. We use the fitted Einasto profile rather than the histogram itself to extract the local number density to avoid sensitivity to the choice of

[2]We note that Ref. [29] does not explicitly state how they reconstruct density profiles at fixed subhalo mass from the extracted VL-II simulation results. The curves shown here are the result of a cubic spline interpolation function fit to $\ln R_{v,\rm max}(\ln M)$ and $\ln v_{c,\rm max}(\ln M)$ in the mass range where VL-II can resolve subhalos, and that we extrapolate to lower masses using a power law fit. The results obtained in this fashion appear to be quite similar to those presented in Ref. [29].

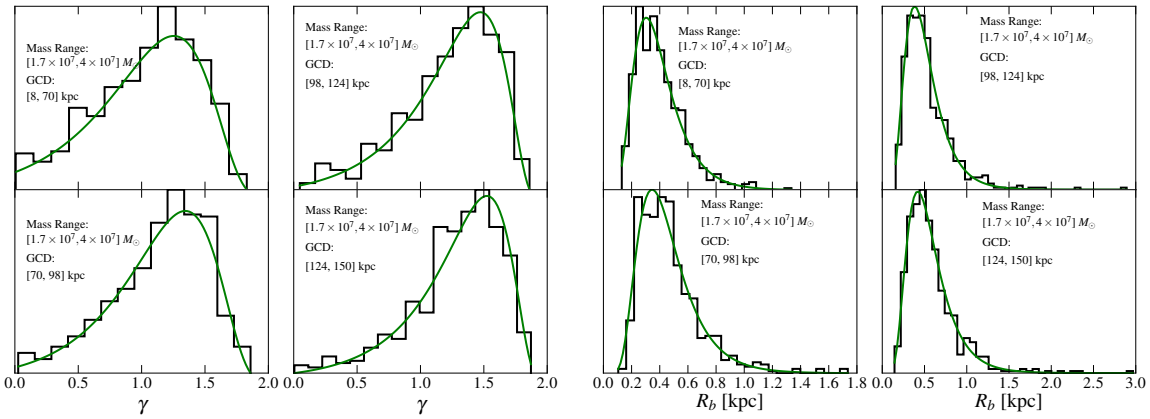

Figure 3. The distribution of the inner slope (left) and exponential scale radius (right) for subhalos in the ELVIS and Via Lactea II simulations, for subhalos with masses in the range of $(2-5)\times10^7 M_\odot$ and at various distances from the Galactic Center (GCD). The green line in each frame depicts the best-fit generalized normal (left) or lognormal (right) distribution.

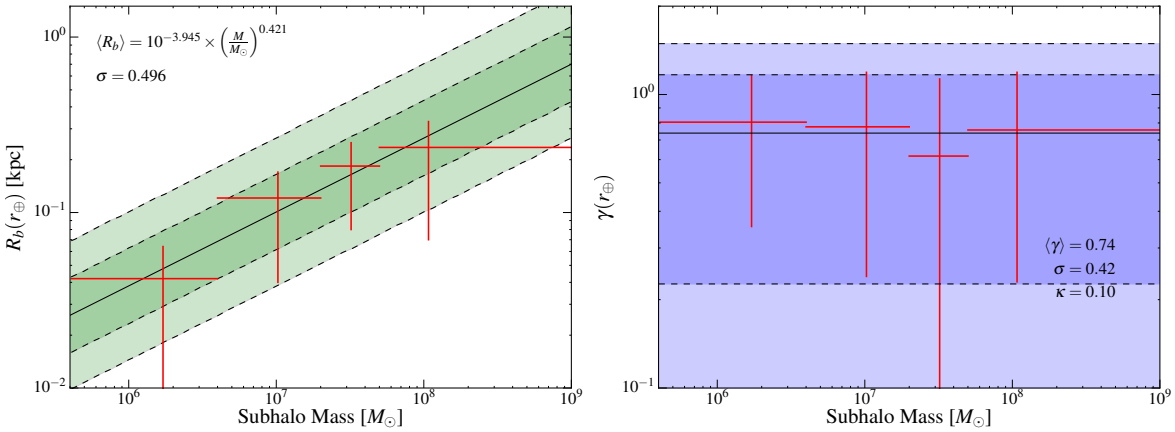

Figure 4. Left: The best-fit power law for the exponential scale parameter, R_b, as a function of subhalo mass, as determined from the ELVIS and Via Lactea II simulation data, for subhalos located 8.5 kpc from the Galactic Center. Right: The mean inner slope, γ, as determined from the ELVIS and Via Lactea II simulation data, for subhalos located 8.5 kpc from the Galactic Center as a function of the subhalo mass. In each frame, the shaded regions depict the 68% and 95% containment contours.

binning. This allows us to derive the following distribution for the local subhalo population:

$$\frac{dN}{dMdV} = \frac{628}{M_\odot\,\mathrm{kpc}^3}\left(\frac{M}{M_\odot}\right)^{-1.9} . \tag{2.6}$$

In the following section, we will use this subhalo distribution, along with the afore described distribution of subhalo density profiles, to calculate the gamma-ray luminosity function of local subhalos, and in turn the number of such subhalos that are predicted to be detectable to Fermi and other gamma-ray telescopes.

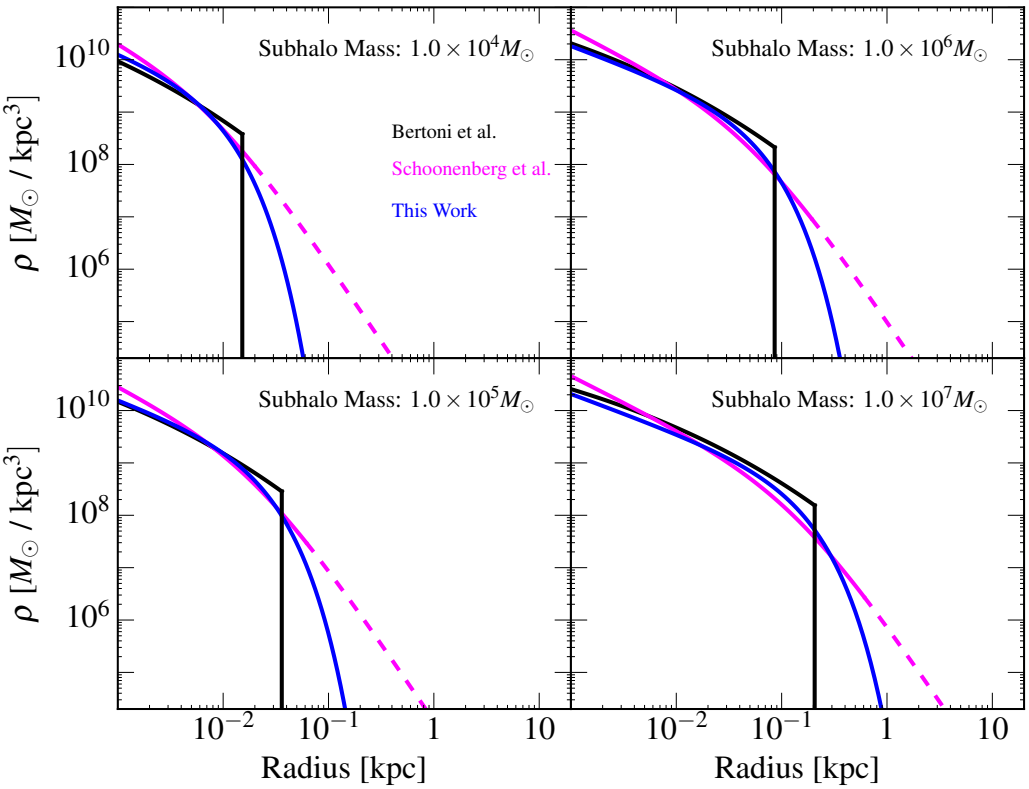
Subhalo Mass: $1.0 \times 10^4 M_\odot$
Subhalo Mass: $1.0 \times 10^6 M_\odot$
Subhalo Mass: $1.0 \times 10^5 M_\odot$
Subhalo Mass: $1.0 \times 10^7 M_\odot$
Bertoni et al.
Schoonenberg et al.
This Work
ρ [$M_\odot$ / kpc^3]
Radius [kpc]

Figure 5. A comparison of the median density profiles adopted in Ref. [27] (black), Ref. [29] (magenta), and as derived in this study (blue) and for subhalos of four different masses.

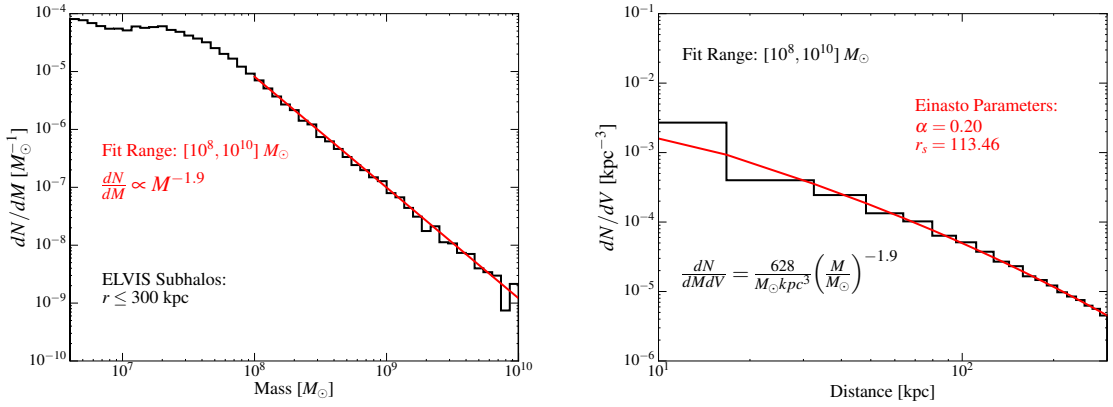

Figure 6. Left: The number of subhalos per unit mass within 300 kpc of the host halo's center as found in the ELVIS suite of simulations. The red line represents the best-fit power-law for subhalos with mass between 10^8 and $10^{10}\,M_\odot$. Right: The number of subhalos per unit volume in the ELVIS simulations for subhalos with masses between 10^8 and $10^{10} M_\odot$. The red line depicts the best-fit Einasto profile for this subhalo distribution. At a distance of 8.5 kpc from the center of the host halo, this corresponds to a local population described by $dN/dMdV = 628\,\mathrm{kpc}^{-3} M_\odot^{-1} \times (M/M_\odot)^{-1.9}$.

3 Detecting Dark Matter Subhalos With Gamma-Ray Telescopes

3.1 Gamma-Rays from Dark Matter Subhalos

A given subhalo will generate a gamma-ray flux that is given by:

$$\Phi_\gamma = \frac{\langle \sigma v \rangle N_\gamma}{8\pi m_\chi^2 D^2} \int \rho^2(r)\, dV, \tag{3.1}$$

where $\langle \sigma v \rangle$ is the dark matter's thermally averaged self-annihilation cross section, N_γ is the number of gamma rays produced per annihilation, m_χ is the dark matter mass, D is the distance to the center of the subhalo, and $\rho(r)$ is the density profile of the subhalo. For a given dark matter mass and annihilation channel, we calculate N_γ using Pythia 8 [56].

From the elements described in the previous section, we can calculate the number of subhalos that yield a gamma-ray flux above a given flux threshold, $\Phi_{\rm Thresh}$:

$$N_{\rm obs} = \Omega \int\int\int\int D^2 \frac{dN}{dM dV} \frac{dP}{d\gamma} \frac{dP}{dR_b} \Theta[\Phi_\gamma(M, D, R_b, \gamma) - \Phi_{\rm Thresh}]\, dM\, dD\, dR_b\, d\gamma, \tag{3.2}$$

where $dN/dMdV$ is the local subhalo number density per unit mass (Eq. 2.6) and $dP/d\gamma$ and dP/dR_b are the generalized normal and lognormal distributions for the parameters γ and R_b, respectively (Eqns. 2.4 and 2.5). The quantity Ω is the solid angle observed, which in the case of $|b| > 20^\circ$ corresponds to $4\pi(1 - \sin 20^\circ)$. To be conservative, we limit the parameter γ to the range of 0 to 1.45, renormalizing the distribution such that $\int_0^{1.45} (dP/d\gamma)\, d\gamma = 1$. In order to compare our calculations to the list of subhalo candidates in the 3FGL gamma-ray source catalog as presented in Ref. [27], we adopt a value of $\Phi_{\rm Thresh} = 7 \times 10^{-10}$ cm^{-2} s^{-1} and consider only photons with energies above 1 GeV. We restrict our attention to subhalos with masses below $10^7\, M_\odot$ to avoid the inclusion of any dwarf galaxies and treat the minimum subhalo mass as a free parameter.

3.2 Placing Constraints on the Dark Matter Annihilation Cross Section

Analyses of the unidentified sources in Fermi's 3FGL catalogue have identified 19 bright ($\Phi_\gamma > 7 \times 10^{-10}$ cm^{-2} s^{-1}), high-latitude ($|b| > 20^\circ$) sources with no evidence of variability and which exhibit a spectral shape consistent with annihilating dark matter [27, 28].[3] In this subsection, we will use the observed number and characteristics of these subhalo candidates to place upper limits on the dark matter annihilation cross section.

Following the approach of Ref. [27], we calculate the χ^2 associated with the fit of a given dark matter model to the spectrum of each subhalo candidate, and define the weighted number of sources to be twice the sum of the p-values associated with the fit (see the left panel of Fig. 10 in Ref. [27]). We then apply Poisson statistics to the weighted number of sources to place a 95% upper limit on the annihilation cross section, for a given value of the dark matter mass and annihilation channel.

In Fig. 7, we plot the upper limit derived for dark matter annihilating to $b\bar{b}$ (purple). The upper (lower) boundary of this band represents the limit obtained assuming a minimum subhalo mass of $10^5\, M_\odot$ ($10^{-5} M_\odot$). We also show in this figure the limits that would have been obtained if no subhalo candidate sources had been detected (zero weighted sources).

[3] The 19 subhalo candidates are the same as those listed in Ref. [27], after removing the five sources that have more recently been associated with emission at other wavelengths [28].

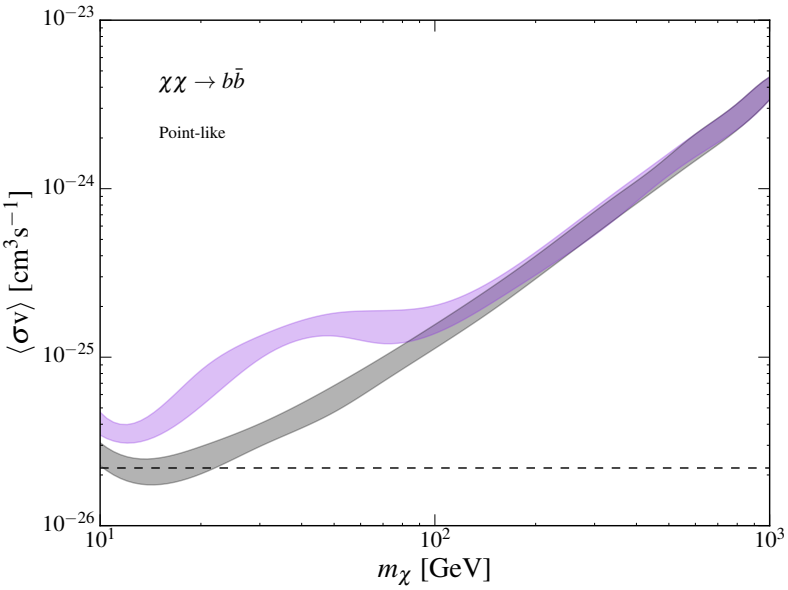

Figure 7. The 95% confidence level upper limit on the cross section for dark matter annihilation to $b\bar{b}$ as derived from the unassociated gamma-ray source population presented in Ref. [27] (purple). Also shown are the limits that would have been derived if no subhalo candidates been observed (grey).

As a benchmark, we plot as a dashed horizontal line the cross section associated with dark matter in the form of a simple thermal relic. In Fig. 8, we show the 95% upper limits for dark matter annihilating to various final states ($b\bar{b}$, $c\bar{c}$, $\tau^+\tau^-$, ZZ or W^+W^-), adopting a minimum mass of either $10^{-5} M_\odot$ (left) or $10^5 M_\odot$ (right).

In Fig. 9, we compare the limits on the annihilation cross section derived in this study to those previously obtained from Fermi's observations of dwarf galaxies (short-dashed blue) [1], the Galactic Center (long-dashed magneta) [3] and the isotropic gamma-ray background (dot-dashed green) [4]. Although the limits from subhalo searches are somewhat weaker than those derived from these other observational targets, they are reasonably competitive and highly complementary.

3.3 Prospects for Detecting Spatial Extension

Thus far our discussion has been restricted to the detection of dark matter subhalos as point-like gamma-ray sources. Of those subhalos detectable by Fermi, however, the most massive and nearby may be discernibly spatially extended, potentially enabling one to distinguish a dark matter subhalo from a pulsar, blazar, or other gamma-ray point source. The unambiguous observation of a spatially extended gamma-ray source with no corresponding emission at other wavelengths would constitute a smoking gun for annihilating dark matter [28].

To quantify the degree of spatial extension of the gamma-ray emission from a dark matter subhalo, we introduce the parameter, σ_{68}, defined as the angular radius which contains 68% of the total photons from the source:

$$\frac{\int_0^{\sigma_{68}} \rho(r)^2 \, dl}{\int_0^{\theta_{\rm max}} \rho(r)^2 \, dl} = 0.68, \tag{3.3}$$

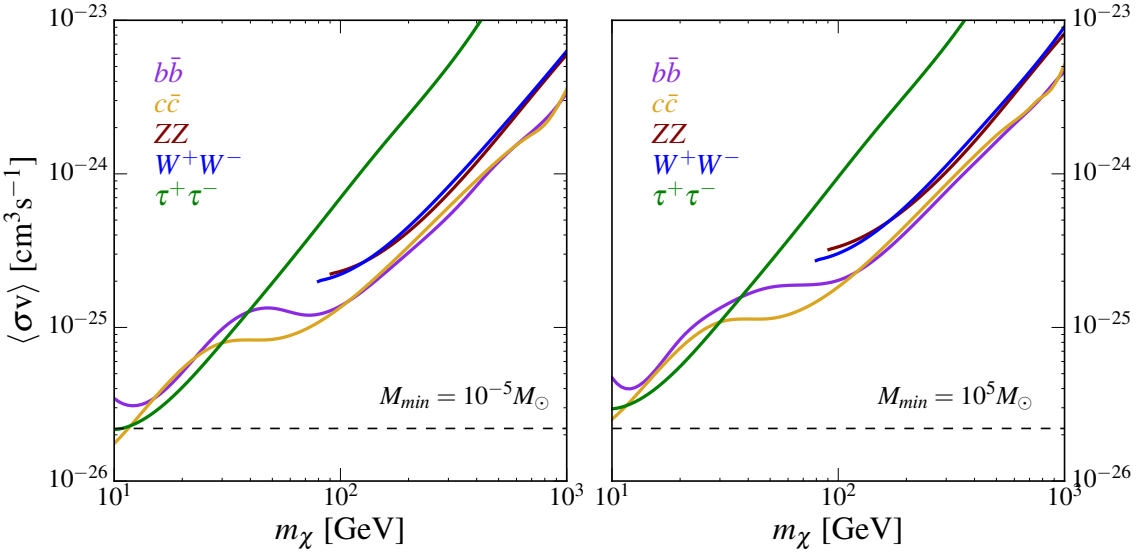

Figure 8. The 95% confidence level upper limit on the dark matter annihilation cross section for various annihilation channels, adopting a minimum subhalo mass of $10^{-5} M_\odot$ (left) or $10^{5} M_\odot$ (right).

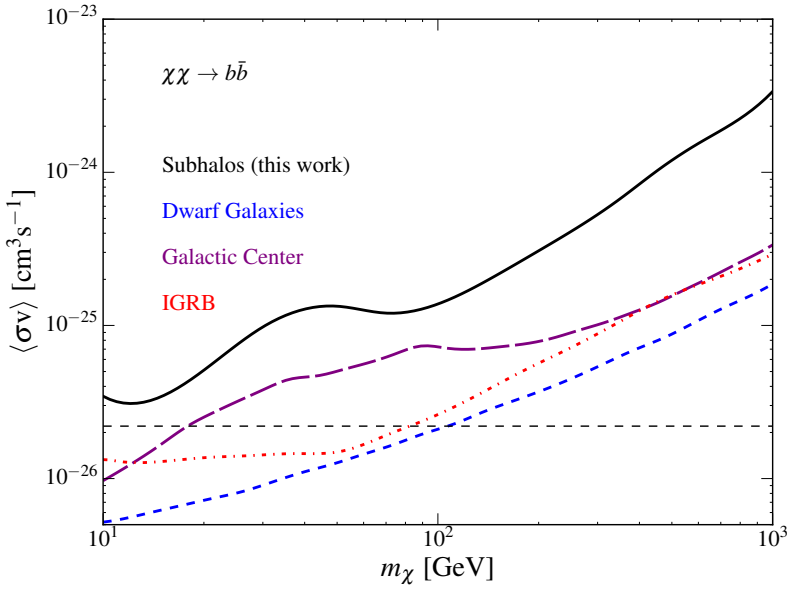

Figure 9. A comparison of the 95% confidence level upper limits on the dark matter annihilation cross section placed from gamma-ray searches for subhalos (solid black) and gamma-ray observations of dwarf galaxies (short-dashed blue) [1], the Galactic Center (long-dashed purple) [3] and the isotropic gamma-ray background (dot-dashed red) [4]. Here we have adopted a minimum subhalo mass of $10^{-5} M_\odot$ and consider the representative case of annihilations to $b\bar{b}$.

where the integrals are performed over the line-of-sight, and $\theta_{\rm max}$ is the angular radius encompassing the full extension of the subhalo. Given the point spread function of Fermi, a bright unassociated source can be potentially identified as spatially extended if $\sigma_{68} \gtrsim \mathcal{O}(0.1^\circ)$ [28]. In the case of bright point-like gamma-ray sources, Fermi can typically place upper limits on

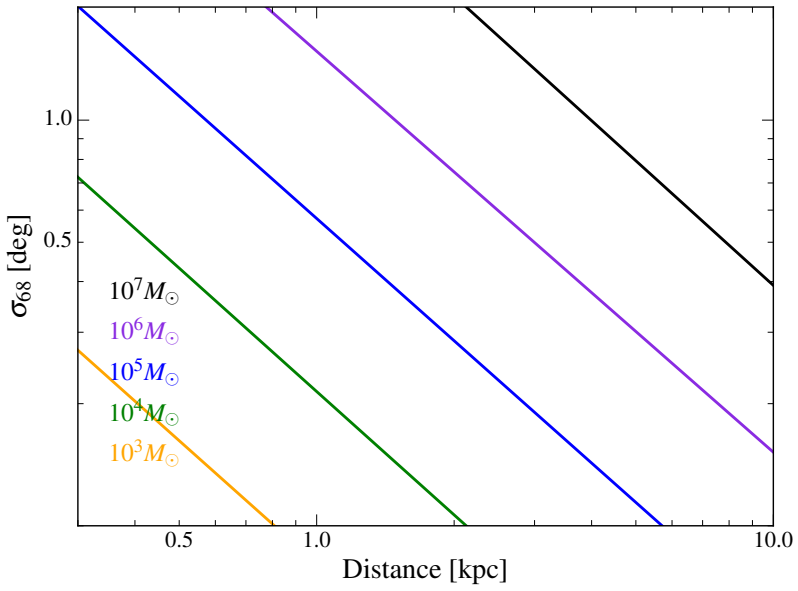

Figure 10. The 68% containment radius, σ_{68}, as a function of the distance to a given subhalo, for five values of the subhalo mass.

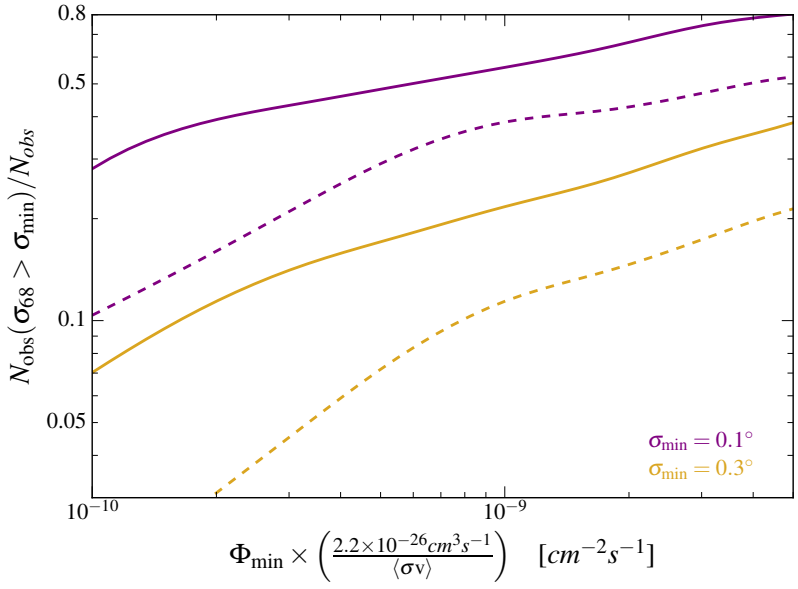

Figure 11. The fraction of subhalos with spatial extension greater than 0.1° (purple) and 0.3° (yellow) as a function of minimum gamma-ray flux (above 1 GeV) and annihilation cross section. Results are shown for a dark matter particle with a mass of 100 GeV (solid) and 10 GeV (dashed), and for the case of annihilations to $b\bar{b}$.

the degree of spatial extension at approximately the same level.

In Fig. 10 we plot σ_{68} as a function of the distance to a given subhalo, for five values of the subhalo mass and assuming a density profile as described by Eq. 2.3 (with R_b and γ set to their median values). This illustrates that in order for an observable subhalo to have

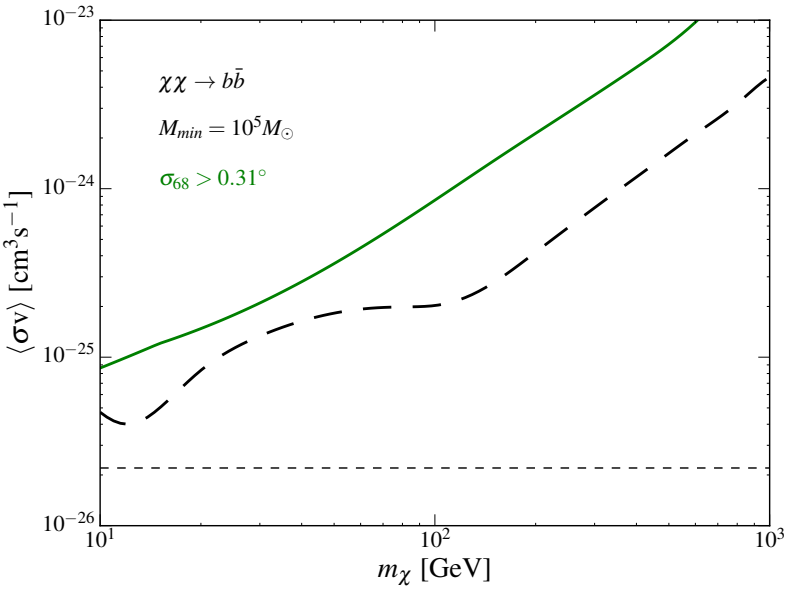

Figure 12. The 95% upper limit on the dark matter annihilation cross section for annihilation into $b\bar{b}$ derived from the non-observation of extended gamma ray sources with a flux above 10^{-9}cm^{-2}s^{-1} and a spatial extension σ_{68} greater than 0.31° (solid green). Shown for comparison are the limits derived from the total number of subhalo candidate sources as depicted in right panel of Fig.8 (dashed black).

potentially discernible extension ($\sigma_{68} \gtrsim 0.1^\circ$), it must be very massive, very nearby, or both.

In Fig. 11, we plot the fraction of subhalos for which $\sigma_{68} > 0.1^\circ$ (purple) or $\sigma_{68} > 0.3^\circ$ (yellow), as a function of the minimum gamma-ray flux and annihilation cross section. Results are shown for dark matter with a mass of 100 GeV (solid) or 10 GeV (dashed), and for the representative case of annihilations to $b\bar{b}$. For dark matter particles in this mass range and with an annihilation cross section of $\langle \sigma v \rangle = 2.2 \times 10^{-26}$ cm^3/s, we predict that approximately 10-20% of subhalos with a gamma-ray flux above 10^{-9} cm^{-2} s^{-1} will be extended at a level of $\sigma_{68} > 0.3^\circ$ and that 40-55% will be extended at $\sigma_{68} > 0.1^\circ$. This can be directly compared to the degree of extension observed among those subhalo candidate sources observed by Fermi.

A recent analysis of the 12 brightest ($\Phi_\gamma > 10^{-9}$cm^{-2}s^{-1}) dark matter subhalo candidates in the 3FGL catalog found that three of these sources prefer a spatially extended morphology at a level of $2\Delta \ln \mathcal{L} > 4$, corresponding to $\gtrsim 2\sigma$ significance [28]. These three sources (3FGL J2212.5+0703, 3FGL J1119.9-2204, and 3FGL J0318.1+0252) were found to be best-fit by extensions of $\sigma_{68} = 0.25^\circ$, 0.07° and 0.15°, respectively. The other nine sources in this sample showed little or no preference for spatial extension. Given the upper limits placed on the spatial extension of these twelve sources, eleven require $\sigma_{68} < 0.3^\circ$ while seven require $\sigma_{68} < 0.1^\circ$ (at the 95% confidence level). Comparing these numbers with the results shown in Fig. 11, we conclude that a scenario in which a large fraction of these subhalo candidate sources are in fact dark matter subhalos is consistent with the predicted distribution of spatial extensions.

According to the analysis of Ref. [28], none of Fermi's subhalo candidates are compatible with extension greater than $\sigma_{68} > 0.31^\circ$. We can use this fact, in conjunction with the predicted distribution of subhalo extensions, to place an upper limit on the dark matter annihilation cross section. In Fig. 12, we plot the 95% upper limit derived from the non-

observation of sources with spatial extension σ_{68} greater than 0.31° (green), for the case of annihilations to $b\bar{b}$ and a minimum subhalo mass of $10^5 M_\odot$. For comparison, we also show in this figure the limit derived from point-like sources (long dashed), assuming the same annihilation channel and minimum subhalo mass. The limit derived from the non-observation of spatially extended sources (with $\sigma_{68} > 0.31^\circ$) is somewhat weaker than that based on the total number of sources observed. That being said, as Fermi and other gamma-ray telescopes continue to accumulate catalogs of dark matter subhalo candidate sources, spatial extension will be essential for distinguishing any subhalo population from other gamma-ray source classes.

3.4 Uncertainties

Thus far in this study, we have not addressed the many uncertainties involved in our calculations. In this section, we will discuss the most important of these uncertainties and their likely impact on our results and conclusions.

We begin by considering the density profiles of the local subhalo population. With an ideal suite of numerical simulations, one could fully resolve the profiles of individual subhalos over a wide range of scales and masses. Current simulations, however, lack the resolution to probe the inner regions such subhalos, making it difficult to distinguish between different functional forms that might describe the distributions of dark matter in these systems. Nevertheless, we are confident that our choice of the density profile parameterization represents an improvement over previous subhalo analyses, and represents approximately the best that can be done with the currently available information. We also note that current simulations are not able to resolve any small-scale structure that may be present *within* a given subhalo, potentially inducing a boost factor to the annihilation rate in a given subhalo. Throughout this analysis, we have conservatively chosen to neglect any boost factors to the annihilation rate.

Arguably, the most significant assumption we have made in our analysis is that the distributions of the parameters γ and R_b which describe the local subhalo population can be safely extrapolated from the distributions describing the subhalos located throughout the larger volume of the host halo. While the distributions of the simulated subhalos do appear to present a clear trend with respect to subhalo location with the host halo, there are simply not enough simulated subhalos in the inner tens of kiloparsecs to extract these parameters and distributions without relying on such an extrapolation. Ideally, as the statistics associated with such simulations continue to improve, we hope to eventually be able to rely exclusively on simulated subhalos located in the inner regions of their host halo, eliminating the need for such an extrapolation.

Similar to how current simulations tell us very little about the small scale structure of dark matter halos and subhalos, they are also not generally capable of revolving the lowest mass subhalos. Below roughly 10^6 to $10^8\,M_\odot$, we are forced to extrapolate the characteristics of the local subhalo population, both in terms of the number density and mass distribution of such subhalos (see the left frame of Fig. 6), and in terms of the distributions of the halo parameters γ and R_b (see Fig. 4). Given that the subhalo distribution extends to masses as low as $\sim 10^{-8}$ to $10^{-3}\,M_\odot$ for typical WIMPs [57–59], even modest departures from this extrapolation can have a non-negligible impact on the predicted number of observable subhalos. To assess the uncertainty associated with this extrapolation, we plot in Fig. 13 the upper limit on the dark matter annihilation cross section when we change the power-law slope of the subhalo mass distribution over the range of -1.8 to -2.0 (in our earlier calculations,

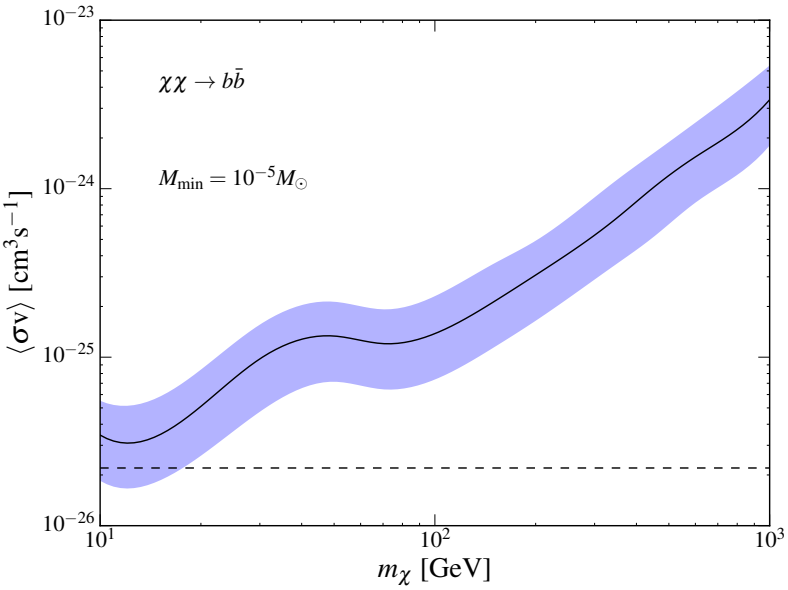

Figure 13. The 95% confidence level upper limit derived on the cross section for dark matter annihilating to $b\bar{b}$, varying the exponent of the subhalo mass distribution $dN/dMdV \propto M^\beta$ (see Eq. 2.6) between $\beta = -1.8$ (upper boundary) and $\beta = -2.0$ (lower boundary), and adopting a minimum subhalo mass of $10^{-5} M_\odot$. The solid black contour represents the limit for our default value of $\beta = -1.9$.

we adopted a value of -1.9; see Eq. 2.6) [46, 47, 60, 61]. Here, we have adopted a minimum subhalo mass of $10^{-5}\, M_\odot$ and again have considered the representative case of annihilations to $b\bar{b}$. This range of limits can vary by a factor of up to $\sim$2 (in either direction) from those presented in the left panel of Fig. 8.

Finally, we would like to emphasize that our results are based on the subhalo populations generated in dark matter-only simulations. As the physical effects of baryons in the Milky Way are not captured in such simulations, our results do not take into account the gravitational potential of our Galaxy's stars, gas and dust. In recent years, there has been considerable progress in understanding the impact of baryons on the evolution of dark matter structure in Milky Way-like systems. In particular, some groups have attempted to capture the effect of the baryonic disk on the evolution of structure in the Milky Way without resorting to a full hydrodynamical treatment, but instead by artificially introducing a disk potential. Some of these simulations (utilizing either an artificial disk potential or a fully hydrodynamical approach) have shown that the presence of such a disk may non-negligibly reduce the local density of subhalos. For example, Refs. [61] and [62] each find that baryonic effects reduce the local number density of subhalos by a factor of approximately $\sim$2. Depending on how these baryonic effects impact the shape of the surviving subhalo density profiles, they could have a wide range of possible impacts on the resulting cross section constraints. Until such hydrodyamical effects are able to be reliably implemented with higher resolution, it will be difficult to assess their impact on the observability of the nearby dark matter subhalo population.

Taking the impact of these various uncertainties together, we conclude that the predicted number of observable subhalos could quite plausibly vary from those values presented here by

a factor of a few in either direction. Only with improvements in the resolution of numerical simulations (both dark matter-only and hydrodynamical simulations) will such predictions be able to be placed on firmer footing, allowing one to establish more robust limits on the dark matter annihilation cross section.

4 Summary and Conclusion

In this paper, we have revisited constraints on the dark matter annihilation cross section derived from searches for dark matter subhalo candidates among Fermi's list of unassociated gamma-ray sources. We have based our calculations on the properties of over $30,000$ subhalos identified within the Via Lactea-II and ELVIS simulations, which we used to constrain the density profiles and the mass distribution of the local subhalo population.

The density profiles of subhalos located within the innermost tens of kiloparsecs of a given host halo are significantly altered as a result of tidal stripping, and in most cases cannot be described by a traditional NFW profile. Instead, we find that these subhalos are well characterized by a power-law profile with an exponential cutoff. While the inner slope of these profiles is largely independent of the subhalo mass (consistently featuring a median value of $\langle\gamma\rangle \simeq 0.74$), the median cutoff radius is a function of mass. Using simulated subhalos from the ELVIS and Via Lactea-II simulations, we fit the distributions of these parameters as a function of the subhalo's mass and distance to the center of the host halo. From this information, we deduce the characteristics of the local subhalo population and calculate the dark matter annihilation rate within this collection of objects, determining the number of subhalos that will appear to Fermi as bright gamma-ray sources.

The limits on the dark matter annihilation cross section that have been derived in this study are somewhat weaker (by a factor of $\sim$2-3) than those presented previously by Bertoni, Hooper and Linden [27], and somewhat stronger than those later presented by Schoonenberg *et al.* [29]. We contend that the approach taken in this study improves upon this previous body of work and accounts for the state-of-the-art in what is currently known from numerical simulations about the local dark matter subhalo population.

We have also calculated the fraction of gamma-ray bright subhalos that are predicted to have discernible spatial extention to a telescope such as Fermi. Such information provides an important test, enabling us to potentially distinguish a dark matter subhalo from a point-like astrophysical source, such as a radio-faint pulsar. We find that for typical WIMPs, roughly 10-50% of gamma-ray bright subhalos will be discernably extended to Fermi, depending on the value of the dark matter's mass and annihilation cross section. This is particularly interesting in light of recent evidence for spatial extension among several of Fermi's subhalo candidates [28]. The results presented here are compatible with the possibility that a significant fraction of these candidate sources could, in fact, be dark matter subhalos.

Although the limits on the dark matter annihilation cross section derived in this study are somewhat weaker than those based on observations of dwarf galaxies, the Galactic Center, and the isotropic gamma-ray background, these strategies are each subject to different uncertainties and limitations, and are thus highly complementary. Furthermore, the future prospects for dark matter subhalo searches using gamma-ray telescopes are particularly promising. In addition to further data that will be collected by Fermi, future space-based gamma-ray missions such as ComPair [63] and e-ASTROGAM [64] are anticipated to significantly improve upon the current point sensitivity at energies below $\sim$1 GeV, likely leading

to the discovery of many new sources, and to the improved characterization of the sources already detected by Fermi.

Acknowledgments. We would like to thank Andrey Kravtsov for very helpful discussions. DH is supported by the US Department of Energy under contract DE-FG02-13ER41958. SW is supported under the University Research Association (URA) Visiting Scholars Award Program, and by a UCLA Dissertation Year Fellowship. Fermilab is operated by Fermi Research Alliance, LLC, under Contract No. DE-AC02-07CH11359 with the US Department of Energy.

References

[1] Fermi-LAT, DES collaboration, A. Drlica-Wagner et al., *Search for Gamma-Ray Emission from DES Dwarf Spheroidal Galaxy Candidates with Fermi-LAT Data*, 1503.02632.

[2] A. Geringer-Sameth, S. M. Koushiappas and M. G. Walker, *A Comprehensive Search for Dark Matter Annihilation in Dwarf Galaxies*, 1410.2242.

[3] D. Hooper, C. Kelso and F. S. Queiroz, *Stringent and Robust Constraints on the Dark Matter Annihilation Cross Section From the Region of the Galactic Center*, *Astropart.Phys.* **46** (2013) 55–70, [1209.3015].

[4] Fermi-LAT collaboration, M. Ackermann et al., *Limits on Dark Matter Annihilation Signals from the Fermi LAT 4-year Measurement of the Isotropic Gamma-Ray Background*, 1501.05464.

[5] M. Di Mauro and F. Donato, *The composition of the Fermi-LAT IGRB intensity: emission from extragalactic point sources and dark matter annihilations*, 1501.05316.

[6] Fermi-LAT collaboration, M. Ajello et al., *Fermi-LAT Observations of High-Energy Gamma-Ray Emission Toward the Galactic Center*, 1511.02938.

[7] T. Daylan, D. P. Finkbeiner, D. Hooper, T. Linden, S. K. N. Portillo et al., *The Characterization of the Gamma-Ray Signal from the Central Milky Way: A Compelling Case for Annihilating Dark Matter*, 1402.6703.

[8] F. Calore, I. Cholis and C. Weniger, *Background model systematics for the Fermi GeV excess*, 1409.0042.

[9] K. N. Abazajian, N. Canac, S. Horiuchi and M. Kaplinghat, *Astrophysical and Dark Matter Interpretations of Extended Gamma-Ray Emission from the Galactic Center*, *Phys.Rev.* **D90** (2014) 023526, [1402.4090].

[10] D. Hooper and T. R. Slatyer, *Two Emission Mechanisms in the Fermi Bubbles: A Possible Signal of Annihilating Dark Matter*, *Phys.Dark Univ.* **2** (2013) 118–138, [1302.6589].

[11] C. Gordon and O. Macias, *Dark Matter and Pulsar Model Constraints from Galactic Center Fermi-LAT Gamma Ray Observations*, *Phys.Rev.* **D88** (2013) 083521, [1306.5725].

[12] K. N. Abazajian and M. Kaplinghat, *Detection of a Gamma-Ray Source in the Galactic Center Consistent with Extended Emission from Dark Matter Annihilation and Concentrated Astrophysical Emission*, *Phys.Rev.* **D86** (2012) 083511, [1207.6047].

[13] D. Hooper and T. Linden, *On The Origin Of The Gamma Rays From The Galactic Center*, *Phys.Rev.* **D84** (2011) 123005, [1110.0006].

[14] D. Hooper and L. Goodenough, *Dark Matter Annihilation in The Galactic Center As Seen by the Fermi Gamma Ray Space Telescope*, *Phys.Lett.* **B697** (2011) 412–428, [1010.2752].

[15] L. Goodenough and D. Hooper, *Possible Evidence For Dark Matter Annihilation In The Inner Milky Way From The Fermi Gamma Ray Space Telescope*, 0910.2998.

[16] I. Cholis, D. Hooper and T. Linden, *Challenges in Explaining the Galactic Center Gamma-Ray Excess with Millisecond Pulsars*, 1407.5625.

[17] S. K. Lee, M. Lisanti, B. R. Safdi, T. R. Slatyer and W. Xue, *Evidence for Unresolved Gamma-Ray Point Sources in the Inner Galaxy*, 1506.05124.

[18] R. Bartels, S. Krishnamurthy and C. Weniger, *Strong support for the millisecond pulsar origin of the Galactic center GeV excess*, 1506.05104.

[19] J. Petrovic, P. D. Serpico and G. Zaharijas, *Millisecond pulsars and the Galactic Center gamma-ray excess: the importance of luminosity function and secondary emission*, *JCAP* **1502** (2015) 023, [1411.2980].

[20] D. Hooper, I. Cholis, T. Linden, J. Siegal-Gaskins and T. Slatyer, *Pulsars Cannot Account for the Inner Galaxy's GeV Excess*, *Phys.Rev.* **D88** (2013) 083009, [1305.0830].

[21] D. Hooper and T. Linden, *The Gamma-Ray Pulsar Population of Globular Clusters: Implications for the GeV Excess*, *JCAP* **1608** (2016) 018, [1606.09250].

[22] T. D. Brandt and B. Kocsis, *Disrupted Globular Clusters Can Explain the Galactic Center Gamma Ray Excess*, *Astrophys. J.* **812** (2015) 15, [1507.05616].

[23] J. Petrovic, P. D. Serpico and G. Zaharijas, *Galactic Center gamma-ray "excess" from an active past of the Galactic Centre?*, *JCAP* **1410** (2014) 052, [1405.7928].

[24] I. Cholis, C. Evoli, F. Calore, T. Linden, C. Weniger et al., *The Galactic Center GeV Excess from a Series of Leptonic Cosmic-Ray Outbursts*, 1506.05119.

[25] E. Carlson and S. Profumo, *Cosmic Ray Protons in the Inner Galaxy and the Galactic Center Gamma-Ray Excess*, *Phys.Rev.* **D90** (2014) 023015, [1405.7685].

[26] S. D. White and C. S. Frenk, *Galaxy formation through hierarchical clustering*, *Astrophys.J.* **379** (1991) 52–79.

[27] B. Bertoni, D. Hooper and T. Linden, *Examining The Fermi-LAT Third Source Catalog In Search Of Dark Matter Subhalos*, *JCAP* **1512** (2015) 035, [1504.02087].

[28] B. Bertoni, D. Hooper and T. Linden, *Is The Gamma-Ray Source 3FGL J2212.5+0703 A Dark Matter Subhalo?*, *JCAP* **1605** (2016) 049, [1602.07303].

[29] D. Schoonenberg, J. Gaskins, G. Bertone and J. Diemand, *Dark matter subhalos and unidentified sources in the Fermi 3FGL source catalog*, *JCAP* **1605** (2016) 028, [1601.06781].

[30] A. Berlin and D. Hooper, *Stringent Constraints on the Dark Matter Annihilation Cross Section From Subhalo Searches with the Fermi Gamma-Ray Space Telescope*, *Phys. Rev.* **D89** (2014) 016014, [1309.0525].

[31] A. V. Belikov, D. Hooper and M. R. Buckley, *Searching For Dark Matter Subhalos In the Fermi-LAT Second Source Catalog*, *Phys.Rev.* **D86** (2012) 043504, [1111.2613].

[32] M. R. Buckley and D. Hooper, *Dark Matter Subhalos In the Fermi First Source Catalog*, *Phys.Rev.* **D82** (2010) 063501, [1004.1644].

[33] Fermi LAT Collaboration collaboration, M. Ackermann et al., *Search for Dark Matter Satellites using the FERMI-LAT*, *Astrophys.J.* **747** (2012) 121, [1201.2691].

[34] H.-S. Zechlin, M. Fernandes, D. Elsaesser and D. Horns, *Dark matter subhalos as Fermi gamma-ray sources and first candidates in the 1FGL catalog*, 1110.6868.

[35] N. Mirabal, V. Frias-Martinez, T. Hassan and E. Frias-Martinez, *Fermi's Sibyl: Mining the gamma-ray sky for dark matter subhaloes*, *Mon.Not.Roy.Astron.Soc.* **424** (2012) L64, [1205.4825].

[36] N. Mirabal, D. Nieto and S. Pardo, *The exotic fraction among unassociated Fermi sources*, 1007.2644.

[37] H.-S. Zechlin and D. Horns, *Unidentified sources in the Fermi-LAT second source catalog: the case for DM subhalos*, *JCAP* **1211** (2012) 050, [1210.3852].

[38] M. Kuhlen, J. Diemand and P. Madau, *The Dark Matter Annihilation Signal from Galactic Substructure: Predictions for GLAST*, *Astrophys.J.* **686** (2008) 262, [0805.4416].

[39] L. Pieri, G. Bertone and E. Branchini, *Dark Matter Annihilation in Substructures Revised*, *Mon.Not.Roy.Astron.Soc.* **384** (2008) 1627, [0706.2101].

[40] E. Baltz, B. Berenji, G. Bertone, L. Bergstrom, E. Bloom et al., *Pre-launch estimates for GLAST sensitivity to Dark Matter annihilation signals*, *JCAP* **0807** (2008) 013, [0806.2911].

[41] V. Springel, S. D. White, C. S. Frenk, J. F. Navarro, A. Jenkins et al., *A blueprint for detecting supersymmetric dark matter in the Galactic halo*, 0809.0894.

[42] V. Springel, S. White, C. Frenk, J. Navarro, A. Jenkins et al., *Prospects for detecting supersymmetric dark matter in the Galactic halo*, *Nature* **456N7218** (2008) 73–80.

[43] S. M. Koushiappas, A. R. Zentner and T. P. Walker, *The observability of gamma-rays from neutralino annihilations in Milky Way substructure*, *Phys.Rev.* **D69** (2004) 043501, [astro-ph/0309464].

[44] A. Tasitsiomi and A. Olinto, *The Detectability of neutralino clumps via atmospheric Cherenkov telescopes*, *Phys.Rev.* **D66** (2002) 083006, [astro-ph/0206040].

[45] Fermi-LAT Collaboration collaboration, F. Acero et al., *Fermi Large Area Telescope Third Source Catalog*, 1501.02003.

[46] J. Diemand, M. Kuhlen, P. Madau, M. Zemp, B. Moore, D. Potter et al., *Clumps and streams in the local dark matter distribution*, *Nature* **454** (2008) 735–738, [0805.1244].

[47] S. Garrison-Kimmel, M. Boylan-Kolchin, J. Bullock and K. Lee, *ELVIS: Exploring the Local Volume in Simulations*, *Mon. Not. Roy. Astron. Soc.* **438** (2014) 2578–2596, [1310.6746].

[48] E. Polisensky and M. Ricotti, *Massive Milky Way Satellites in Cold and Warm Dark Matter: Dependence on Cosmology*, *Mon. Not. Roy. Astron. Soc.* **437** (2014) 2922–2931, [1310.0430].

[49] Planck collaboration, P. A. R. Ade et al., *Planck 2015 results. XIII. Cosmological parameters*, 1502.01589.

[50] N. Mirabal, E. Charles, E. C. Ferrara, P. L. Gonthier, A. K. Harding, M. A. Snchez-Conde et al., *3FGL Demographics Outside the Galactic Plane using Supervised Machine Learning: Pulsar and Dark Matter Subhalo Interpretations*, *Astrophys. J.* **825** (2016) 69, [1605.00711].

[51] S. Kazantzidis, L. Mayer, C. Mastropietro, J. Diemand, J. Stadel and B. Moore, *Density profiles of cold dark matter substructure: Implications for the missing satellites problem*, *Astrophys. J.* **608** (2004) 663–3679, [astro-ph/0312194].

[52] J. Penarrubia, J. F. Navarro and A. W. McConnachie, *The Tidal Evolution of Local Group Dwarf Spheroidals*, *Astrophys. J.* **673** (2008) 226, [0708.3087].

[53] A. Moline, M. A. Sanchez-Conde, S. Palomares-Ruiz and F. Prada, *Characterization of subhalo structural properties and implications for dark matter annihilation signals*, 1603.04057.

[54] V. Springel, J. Wang, M. Vogelsberger, A. Ludlow, A. Jenkins, A. Helmi et al., *The Aquarius Project: the subhalos of galactic halos*, *Mon. Not. Roy. Astron. Soc.* **391** (2008) 1685–1711, [0809.0898].

[55] G. Despali and S. Vegetti, *The impact of baryonic physics on the subhalo mass function and implications for gravitational lensing*, 1608.06938.

[56] http://home.thep.lu.se/~torbjorn/Pythia.html.

[57] S. Profumo, K. Sigurdson and M. Kamionkowski, *What mass are the smallest protohalos?*, *Phys. Rev. Lett.* **97** (2006) 031301, [astro-ph/0603373].

[58] T. Bringmann, *Particle Models and the Small-Scale Structure of Dark Matter*, *New J. Phys.* **11** (2009) 105027, [0903.0189].

[59] J. M. Cornell, S. Profumo and W. Shepherd, *Kinetic Decoupling and Small-Scale Structure in Effective Theories of Dark Matter*, *Phys. Rev.* **D88** (2013) 015027, [1305.4676].

[60] J. Diemand, M. Kuhlen and P. Madau, *Dark matter substructure and gamma-ray annihilation in the Milky Way halo*, *Astrophys.J.* **657** (2007) 262–270, [astro-ph/0611370].

[61] T. Sawala, P. Pihajoki, P. H. Johansson, C. S. Frenk, J. F. Navarro, K. A. Oman et al., *Shaken and Stirred: The Milky Way's Dark Substructures*, 1609.01718.

[62] R. Errani, J. Penarrubia, C. F. P. Laporte and F. A. Gomez, *The effect of a disc on the population of cuspy and cored dark matter substructures in milky way-like galaxies*, *ArXiv e-prints* (aug, 2016) , [1608.01849].

[63] A. A. Moiseev et al., *Compton-Pair Production Space Telescope (ComPair) for MeV Gamma-ray Astronomy*, 1508.07349.

[64] V. Tatischeff et al., *The e-ASTROGAM gamma-ray space mission*, *Proc. SPIE Int. Soc. Opt. Eng.* **9905** (2016) 99052N, [1608.03739].